

LARGE EMITTANCE BEAM MEASUREMENTS FOR COMET PHASE-I

A. Kurup, I. Puri, Y. Uchida, Y. Yap, Imperial College London, UK

R. B. Appleby, S. Tygier, The University of Manchester and the Cockcroft Institute, UK

R. D'Arcy, A. Edmonds, M. Lancaster, M. Wing, UCL, UK

Abstract

The COMET experiment will search for very rare muon processes that will give us an insight into particle physics beyond the Standard Model. COMET requires an intense beam of muons with a momentum less than 70 MeV/c. This is achieved using an 8 GeV proton beam; a heavy metal target to primarily produce pions; a solenoid capture system; and a curved solenoid to perform charge and momentum selection.

Understanding the pion production yield and transport properties of the beam line is an important part of the experiment. The beam line is a continuous solenoid channel, so it is only possible to place a beam diagnostic device at the end of the beam line. Building COMET in two phases provides the opportunity to investigate the pion production yield and to measure the transport properties of the beam line in Phase-I. This paper will demonstrate how this will be done using the experimental set up for COMET Phase-I.

INTRODUCTION

The COherent Muon to Electron Transition (COMET) experiment aims to measure the conversion of muons to electrons, in the presence of a nucleus, with an unprecedented sensitivity of $< 10^{-16}$. The details of the COMET Phase-I beam line can be found in [1] and Fig. 1 shows a schematic of the beam line. COMET Phase-I will provide an invaluable opportunity to make measurements to characterise the beam line, since this cannot be done after the full COMET beam line has been constructed. The

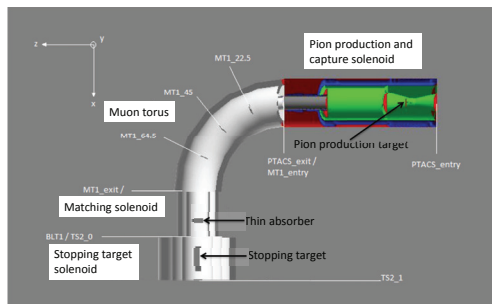


Figure 1: Schematic layout of COMET Phase-I.

COMET beam line is a large aperture, continuous solenoid channel, and accurate simulation of transport properties is dependent on knowing the field precisely. It will be difficult to measure this as the solenoids will be closely coupled and there will be no option for placing complex beam diagnostic equipment between cryostats. In addition to this, the beam will occupy the whole aperture and will consist

of multiple species. This means it will be very difficult to measure the transport properties along the length of the beam line after it has been installed.

In order to get an understanding of the performance of the beam line, it will be possible to vary certain parameters of the magnets, such as magnetic field strength, and to measure a corresponding effect at the end of the transport channel. By making several measurements with different types of changes it may be possible to characterise the performance of the beam line in order to understand the background processes that can create electrons that could be mistaken to have come from muon to electron conversion.

In addition to this, there is some uncertainty as to the precise composition of the beam due to different models giving different predictions for the production of hadrons in this momentum range. It will therefore be important to be able to measure the production rates and spectra in order to understand potential sources of background particles.

HADRON PRODUCTION SIMULATION

MARS [2] is currently used to produce the initial beam which is then tracked through the beam line using Geant4 [3]. There are however significant discrepancies between models that simulate the production of hadrons from an 8 GeV proton beam colliding with a high-Z metal target. Figure 2 shows the momentum distribution of muons and pions produced using MARS and different models in Geant4. The muon and pion momentum distributions produced by FLUKA [4] are shown in Fig. 3.

It would be good to measure the precise particle flux produced by the proton beam collisions but this would require a very sophisticated detector system. By changing the transport properties of the beam line it may be possible to infer the species content of the beam using a relatively simple detector.

FIELD VARIATIONS

One simple way to vary the transport characteristics of the beam line is to vary the magnetic field. Two options were considered in these simulations: changing the solenoid field of the capture solenoid surrounding the pion production target; and changing the dipole field of the muon torus.

Figure 4 shows the effect of changing the capture solenoid field on the momentum distribution of negatively charged pions and muons and Fig. 5 shows the effect on the number of high-momentum negatively and positively charged particles at the entrance of the muon torus.

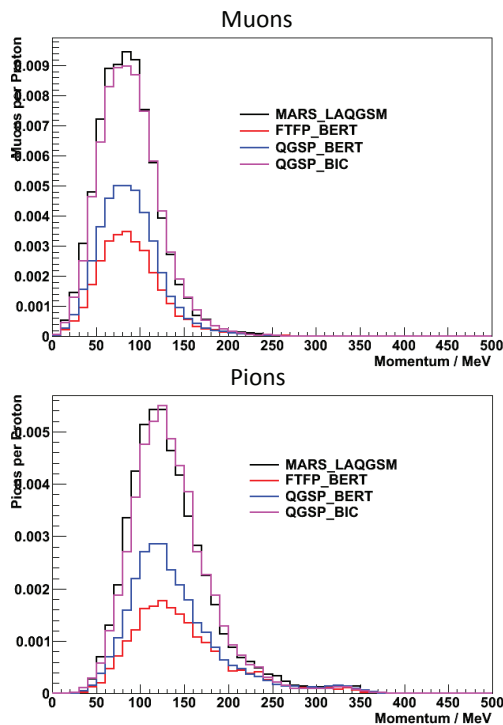


Figure 2: Momentum distribution of muons (top) and pions (bottom) at the entrance of the muon torus produced by different MARS and Geant4 models. The vertical scale is normalised to the number of primary protons used in the simulation.

High-momentum is defined as: pions with a momentum greater than 80 MeV/c; muons with a momentum greater than 75 MeV/c; and electrons/positrons with a momentum greater than 100 MeV/c. Figure 6 shows the ratio of pions to muons for high- and low-momentum particles. By changing the dipole field the high-momentum pion to muon ratio after the muon torus can be affected. Thus by making momentum measurements it is possible to understand the high-momentum pion content of the beam.

ABSORBER

The particle composition of the beam can also be changed by placing an absorber material in the beam line as particles with the same momentum but different masses will interact differently with the absorber. Simulations were performed using a simple absorber that filled the whole aperture but was thin in the direction of the beam. The location of the absorber is shown in Fig. 1. Changing the absorber thickness and material was then investigated. Figure 7 shows the momentum distribution for muons after the absorber for different tungsten absorber thicknesses and Fig. 8 shows the percentage of pions, muons and electrons absorbed by the absorber (this also includes the production of secondary electrons). This was repeated with an aluminium absorber, see Figs. 9 and 10.

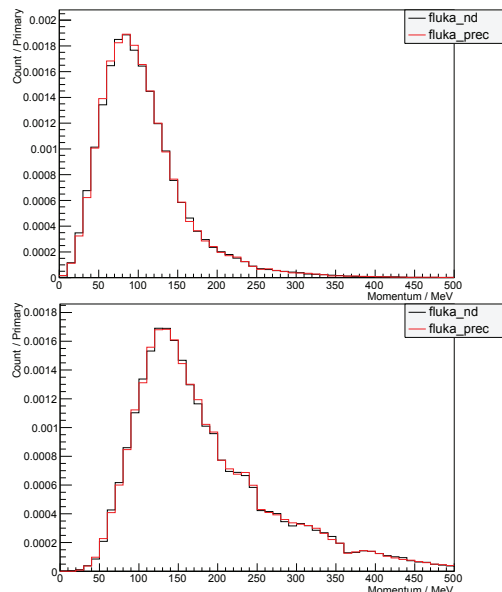


Figure 3: Momentum distribution of muons (top) and pions (bottom) at the entrance of the muon torus produced by the FLUKA default (fluka_nd) and precision (fluka_prec) models. The vertical scale is normalised to the number of primary protons used in the simulation.

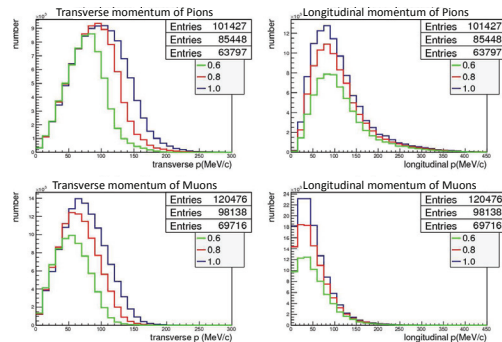


Figure 4: Effect of scaling the capture solenoid field on the momentum distribution of negatively charged pions and muons at the entrance of the muon torus.

CONCLUSIONS

By changing the beam line, as described in the previous sections, it is possible to alter the momentum distribution and species composition of the beam. Thus, making momentum measurements with a simple detector will provide a better understanding of the background process that could fake the muon to electron conversion signal.

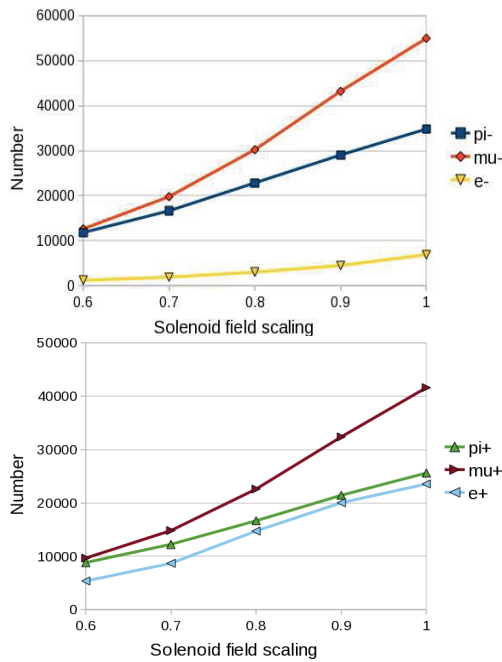


Figure 5: Effect of scaling the capture solenoid field on the number of negatively charged (top) and positively charged (bottom) particles at the entrance of the muon torus.

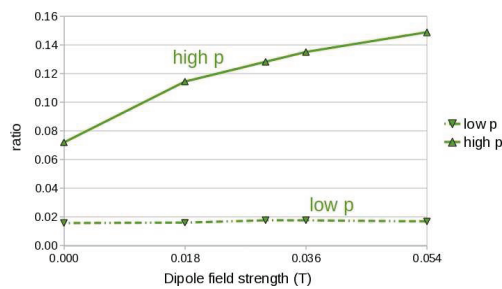


Figure 6: The negatively charged pion to muon ratio for high-momentum and low-momentum particles after the muon torus for different dipole fields.

REFERENCES

[1] A. Kurup, I. Puri, Y. Yap, R. Appleby, S. Tygier, A. Edmonds, "Optimisation of the Beam Line For Comet Phase-I", in these proceedings.
 [2] N. Mokhov, S. I. Striganov, "MARS15 Overview.", Fermilab-Conf-07-008-AD, 2007.
 [3] S. Agostinelli et al., Nucl. Inst. and Meth. A **506** (2003) 250-303.
 [4] G. Battistoni, S. Muraro, P. R. Sala, F. Cerutti, A. Ferrari, S. Roesler, A. Fassio, J. Ranft, "The FLUKA code: Description and benchmarking.", Proc. of the Hadronic Shower Simulation Workshop 2006, M. Albrow, R. Raja eds., AIP Conference Proceeding 896, 31-49, (2007).

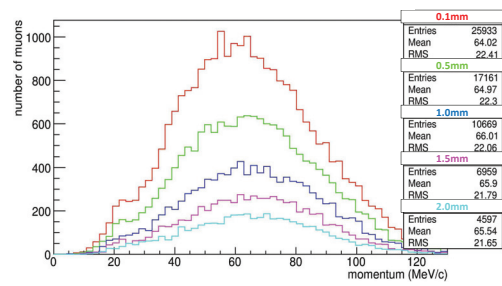


Figure 7: Momentum of muons after the tungsten absorber for different thicknesses.

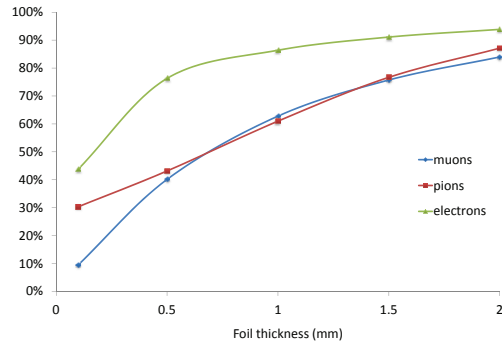


Figure 8: Percentage of pions, muons and electrons stopped by the tungsten absorber for different thicknesses.

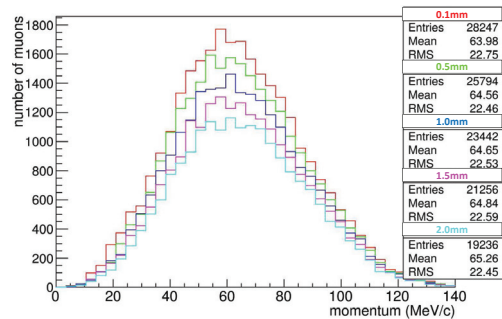


Figure 9: Momentum of muons after the aluminium absorber for different thicknesses.

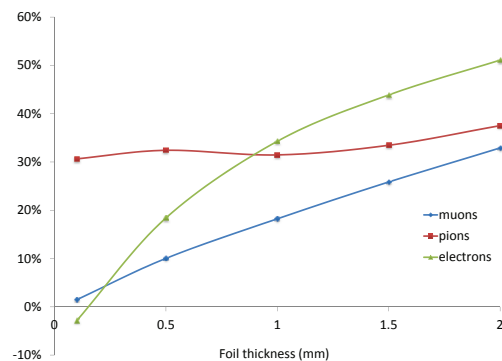


Figure 10: Percentage of pions, muons and electrons stopped by the aluminium absorber for different thicknesses.